Conductive probe AFM study of Pt-thiol and Au-thiol contacts in metal-molecule-metal systems

Chang Min Kim and John Bechhoefer

Additional information on J. Chem. Phys.

Conductive probe AFM study of Pt-thiol and Au-thiol contacts in metal-molecule-metal systems

Chang Min Kim and John Bechhoefer[a)]
Department of Physics, Simon Fraser University, Burnaby, British Columbia V5A 1S6, Canada

The charge transport mechanism between 1,8-octanedithiol (ODT, $C_8H_{16}S_2H_2$) and platinum and gold electrodes is studied by breaking bonds between single ODT molecules and atomic metal junctions using conductive probe atomic force microscopy. Histograms of conductance values show peaks that are obscured by background processes that differ from the metal-molecule-metal conduction path of interest. We introduce a new method to reduce greatly such backgrounds by dividing by a 1-octanethiol (OMT, $C_8H_{17}SH$) reference histogram, without data selection. The method reveals three series of conductance values for both platinum and gold contacts, which we associate with geometrically different configurations between thiol and metal atoms. The ordering of conductance values, Pt-ODT-Pt > Pt-ODT-Au> Au-ODT-Au, is consistent with a relative dependence on both the number of electron channels and the density of states. © 2013 American Institute of Physics. [http://dx.doi.org/10.1063/1.4773436]

I. INTRODUCTION

Inspired by the potential to use single molecules as electronic components,[1,2] there has been intense interest in understanding electron transport mechanisms through various molecules, including ones with conjugated[3–6] and saturated molecules.[7–11] Especially for saturated molecules, many experimental[7–10,12–22] and theoretical[23,24] studies have examined charge-transport mechanisms through a single molecule, especially in the metal-linker-molecule-linker-metal configuration. The issue of charge transport across metal-molecule interfaces is of particular interest, as the interface plays a crucial role in the overall conductance of metal-molecule-metal systems.[12,25–30]

The chemical ligands wiring a molecule to metal electrodes that have been most studied include thiols (–SH),[9,17,20–22,31,32] amines (–NH_2),[15,33–35] carboxyls (–COOH),[34] dimethyl phosphines (–PMe_2),[35] and, recently, selenols (–SeH).[36] Studies of these wiring ligands have shown that interface properties significantly affect both the physical structure and the electronic coupling at the interface. Logically, if the chemical ligand affects binding properties, the type of material used as an electrode will also affect the interface properties. In particular, "interface states," the states forming in the metal electrode when a metal binds to molecular ligands, can significantly affect the electronic behavior of the total metal-molecule-metal system.[23,24,37] However, there have been few studies of the conductance of molecules using electrode materials other than gold.[38,39]

In this paper, we study the conduction mechanisms at the interface between the technologically important thiol ligand and metal electrodes. Previous studies on such systems have been complicated by the strong ligand bond, which leads to complex behavior in conductance histogram measurements. Here, we introduce a way to reduce such backgrounds significantly, allowing a clearer analysis of the underlying conduction mechanisms. We apply this method to the study of the role of the substrate electrode material (Au or Pt) in single-molecule conductance experiments, studying Au-molecule-Au, Au-molecule-Pt, and Pt-molecule-Pt configurations. Comparing conductance values for different electrodes suggests that the conduction mechanisms at the junction depend both on the number of accessible electron channels and the density of states.

We investigate transport mechanisms at the interface using a simple alkanedithiolate, 1,8-octanedithiol, $C_8H_{16}(SH)_2$, or ODT. By comparing its conductance values in settings with different combinations of gold (Au) and platinum (Pt) electrodes, we analyze how the electronic and structural properties at metal electrodes relate to the conduction mechanisms of a single ODT molecule. In our study, we used a break-junction technique based on conductive-probe atomic force microscopy (CP-AFM).[9,40] The break-junction method consists of making and then breaking a metal-molecule-metal junction repeatedly while placing a potential difference (bias voltage) between probe tip and substrate. This technique is useful for investigating the transport characteristics of the junction between a thiol ligand and a Pt or Au electrode, as its structural configurations change, while the junction elongates. Pt and Au have similar structural and electronic properties but differ in lattice binding energy and the number of cohesive electrons. We can thus evaluate the role of binding energy and binding electrons in the electrode materials by comparing the conductances of each configuration.

II. EXPERIMENTAL PROCEDURES

A. Apparatus

For the break-junction experiments, we used a commercial atomic force microscope (Asylum Research, Model

---

a)Electronic mail: johnb@sfu.ca.

(a)

(b)

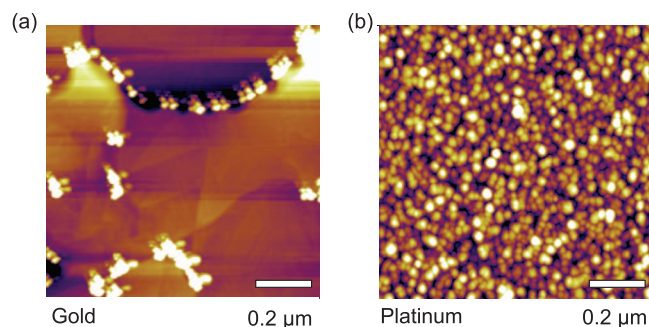Gold   0.2 μm   Platinum   0.2 μm

FIG. 1. The AFM topography of (a) Au (111) and (b) Pt. The grain size of platinum is far smaller than that of gold because of deposition conditions and the higher melting point of Pt. Scale bar shows 0.2 μm in both cases.

MFD-3D) with a closed liquid cell (Asylum Research Part No. 939.009), made of PEEK (polyether ether ketone, a chemically resistant plastic), a glass window, sealed hole for a metal electrodes for contact, a flexible viton membrane, and O-rings. These were cleaned thoroughly in ethanol and deionized (DI) water by sonication. They were then dried with filtered pure N$_2$ gas (99.99%, Praxair Co.) just before each experiment to prevent contamination.

We used an AFM cantilever holder with a dual-gain amplifier (Dual Gain ORCA). This amplifier collects current through the tip simultaneously with a high-gain (1 nA/V) and a low-gain (1 μA/V) I–V converter. The transformed signal is converted to a digital signal by a 16 bit A/D converter at 200 kHz. The maximum acquisition rate we could select via software was 50 kHz.

B. Substrates

We prepared gold and platinum thin films on mica and plasma-cleaned glass slide substrates, to serve as metal electrodes for metal-molecule-metal systems. The platinum substrates were prepared by electron-beam evaporation on glass slides (Fisher Scientific, thickness # 2) at 4D LABS at Simon Fraser University. First, glass slides were cleaned by *in situ* Ar-plasma at 100 W, 4 × 10^{-3} torr, for 5 min. Then a Cr adhesion layer (≈ 5 nm) and a Pt layer (≈ 200 nm) was deposited at 0.7 to 0.9 Å/s. The evaporations were performed by Chris Balicki (4D LABS).

Gold was thermally evaporated (99.99%, PAMP S.A.) on freshly cleaved mica at a substrate temperature of 380 ± 5 °C. The deposition rate was 0.5 Å/s, and the base pressure was less than 2 × 10^{-6} torr. We kept the substrate temperature at 380 °C for more than 7 h before and 3 h after evaporation to remove impurities from the mica surface and to give enough time for adsorbed gold atoms to move and create a flatter surface.

As we see in Fig. 1, the gold on mica has large, flat grains, but the platinum surface has small grains. This difference in flatness results from different deposition conditions and the much higher melting temperature of platinum (1770 °C) relative to gold (1065 °C).

After evaporation, films were kept in a vacuum desiccator. Just before each experiment, every film was cleaned for 20 min by UV/O$_3$ cleaner (Novascan, model: PSD-UV) and

briefly annealed using a butane flame torch. When annealing the film, we observed the outer flame in the dark so that the film glowed dimly with an orange color for 1 min. We carefully waved the flame up and down at about 1 Hz in order not to roughen the surface. The important point is that since gold does not wet mica, liquid gold gathers into small droplets, creating a rough surface. Thus, while annealing allows surface to become smoother, melting roughens it. The procedure described above thus tries to ensure uniform temperature to avoid any local melting.

We used Au-Cr and Pt-Ti coated cantilevers with spring constants ranging from 0.6 nN/nm to 36 nN/nm (nominal values from the manufacturer). All the cantilevers were cleansed in UV/O$_3$ cleaner for 20 min.

C. Chemicals

We used 1 mM of ODT solution of hexane for making ODT SAMs and performing break-junction measurements. 1,8-octanedithiol (ODT) was used as purchased (98%, Alfa Aesar). ODT is composed of eight CH$_2$ groups with thiols (–SH) at each end of the molecule. ODT is a good model system for investigating of conductance properties of contacts, for several reasons. First, the sulfur atom has a strong affinity for the noble metals, including gold and platinum. Second, because alkanes have large HOMO-LUMO gaps, electron tunneling is the main conduction mechanism through ODT. This property enables us to consider the sole effect of the contact in isolation from the complexity of molecule itself. Finally, since ODT is one of the most widely studied alkanedithiols, its conductance has already been measured. These properties led us to choose ODT to investigate the metal-ligand contact.

For 1-octanethiol (C$_8$H$_{17}$SH or OMT) was purchased (96%, Alfa Aesar). OMT is composed of 8 carbon atoms with a thiol ligand at one end and a hydrogen atom at the other. For the OMT break-junction experiments, we made an OMT 1 mM solution in methanol, immersed each Au and Pt sample in solution for 24 h to make dense SAMs, and rinsed by ethanol.

For a solvent for the ODT solution, we tested hexane (EMD, 98.5%, HPLC grade), 1,2,4-trichlorobenzene (TCB, Alfa Aesar, 99%, spectroscopy grade), and toluene (Anachimia, 99.5%, reagent grade). We preferred hexane because, among the solvents tested, it had the least effect on the viton membrane of the liquid cell. With other solvents, we hardly ever saw the saturated currents (=10 μA) that indicate direct contact between the tip and the metal substrate. In addition, we saw many steps or smooth decrease in current-distance curves, which we believe are artifacts because the steps do not correspond to a known conductance of ODT. A smooth decrease of a current means the existence of layers that conduct current other than a ligand-to-ligand conduction through ODT.

We believe that the observed contamination is due to the greater reactivity of toluene and TCB relative to hexane. For the case of TCB, since the Pt electrode can bind the Cl of TCB, we are not able to measure conductance of ODT, because of a layer of TCB.
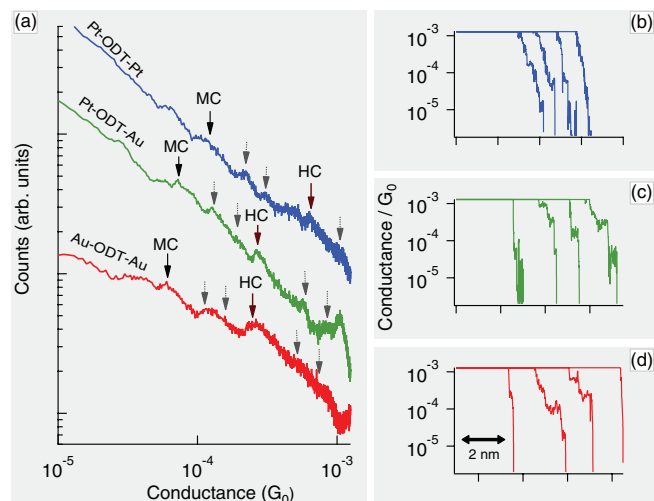
FIG. 2. (a) Conductance histograms of ODT for the Au-ODT-Au, Au-ODT-Pt, and Pt-ODT-Pt configurations at $V_b = 0.1$ V. Solid arrows indicate primary MC and HC conductance peaks. Dashed arrows indicate integer multiples of the primary conductance peaks. Typical current-distance curves for the (b) Pt-ODT-Pt, (c) Pt-ODT-Au, and (d) Au-ODT-Au configurations. Horizontal data lines in (b)–(d) reflect saturation of the transimpedance amplifier.

In addition, the current noise level of hexane itself is the lowest among the three solvents. We ascribe this observation to its low dielectric constant (1.88 at 25 °C, vs. toluene 2.38, trichlorobenzene 2.24, at 20 °C). In general, the dielectric constant of solvents are related to the solvent polarity. A high polarity can result in fragmentation of a solvent molecule resulting from the high electric field concentration between the AFM tip and the metal surface ($\approx 10^8$ V/m). Hexane has the disadvantage of a higher vapor pressure; however, the closed liquid cell chamber minimized evaporation. In practice, we could perform measurements for several hours.

III. RESULTS

We carried out break-junction measurements for three configurations: Au-ODT-Au, Pt-ODT-Au, and Pt-ODT-Pt. We show results of the measurements in Fig. 2 and Table I.

Figure 2 shows conductance histograms for the three configurations. In the raw data, it is difficult to distinguish conductance peaks from background noise. In all cases, we observe small peaks on a power-law background. To understand why the background level is so high relative to the conductance signal, we recall that one of the difficulties in measuring conductances of single molecules using the break-junction technique is the variation of conductances resulting

from the many possible states of the microscopic molecular binding structure between the electrode and the molecule.[41–43] This variation results from multiple possibilities for thiol-gold bonds[17,41,44] and from multiple conformations of the molecule (e.g., *trans* and *gauche* isomers).[22,42,43] In addition to the various microscopic binding conformations, many other mechanisms contribute to this high background, including hydrogen conduction between tip and Au substrate while forming tip-molecule binding,[45] tunneling through solvent,[46] and intermolecular chain-to-chain tunneling.[47–49]

In an effort to improve the signal-to-background (S/B) ratio of conductance histograms, Venkataraman *et al.*[15,35] substituted amine binding groups for thiols. Using break-junction measurements, they attributed the low S/B ratio of conventional histograms to the existence of two possible binding sites for thiol ligands, where multiple binding possibilities can lead to a broad range of conductance variations.[41] Since the amine binding group has only one binding site, the primary peak is higher relative to the background, despite the higher contact resistance (lower conductance) of the amine ligand.[15,35,50]

A. Background reduction using a control experiment

Although break-junction experiments using thiol groups are problematic because of the large background, studies based on thiol groups remain interesting, as they are used in a wide variety of technological applications. Attempts to reduce the histogram background on thiol-based systems have been based on subtracting a background histogram compiled on bare gold or on cutting off the region below current steps that show the primary peaks of alkanedithiol molecules.[50,51] Here, we present a new method to reduce the noise and complexity of conductance histograms that makes peaks stand out, without subjective data selection.

First, we note that the histogram baselines are almost linear in log-log plots. That is, the baselines show an approximate power-law dependence[15,41,50,52] that is possibly the result of intermolecular chain-to-chain tunneling,[47–49] with the contacts coming from various loads produced by the AFM tip on the SAMs.[53–56]

Second, since OMT is structurally the same as ODT except for a hydrogen atom at one end instead of a thiol, the same intermolecular chain-to-chain tunneling processes will be present. We thus compile, as a reference, a conductance histogram where we substitute an OMT for ODT. We then divide the ODT histogram by the reference OMT histogram, thereby removing almost all the background due to transport

TABLE I. Conductance values for Au-ODT-Au, Pt-ODT-Au, and Pt-ODT-Pt systems. The values are estimated from histogram peak locations after background removal using an OMT control experiment for $V_b = 0.1$ V. Conductances are in units of $10^{-4} G_0$.

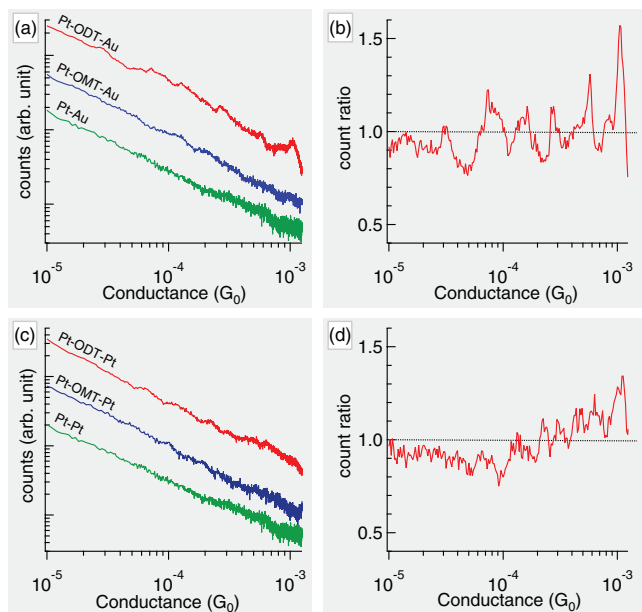| Configuration (tip-molecule-substrate)	Au-ODT-Au	Pt-ODT-Au	Pt-ODT-Pt
HC ($\times 10^{-4} G_0$)	2.55 ± 0.2	2.8 ± 0.4	6.3 ± 0.7
MC ($\times 10^{-4} G_0$)	0.55 ± 0.05	0.73 ± 0.27	1.25 ± 0.2
LC ($\times 10^{-4} G_0$)	(0.12)[a]	0.24 ± 0.14	0.64 ± 0.23

[a] Measured at $V_b = 0.2$ V.

FIG. 3. Background removal of histograms for the Pt-ODT-Au and Pt-ODT-Pt configurations for $V_b = 0.1$ V. (a), (b) Pt-ODT-Au case (c), (d) Pt-ODT-Pt case. In (a) and (c), the top curve is the original ODT histogram, while the middle and lower histograms (blue and green, offset for clarity) correspond to control experiments performed in hexane solvent on a bare gold substrate and on an OMT self-assembled monolayer. (b) and (d) ODT histograms divided by OMT histogram.

mechanisms other than the ligand-to-ligand transport mechanism that we wish to study. We note that on a log-log plot, division "subtracts" a background contribution. We normalize the histograms by multiplying by the ratio of total counts in each histogram, N_{OMT}/N_{ODT}, so that the average level of counts in each bin is equal to one. The broad features of histogram ratios are robustly reproducible.

Figure 3 shows the result of this procedure, with Fig. 3(a) showing the original Pt-ODT-Au, Pt-OMT-Au, and Pt-Au histograms from top to bottom. In Fig. 3(b), we show the result of dividing the original histogram in Fig. 3(a) by the Pt-OMT-Au histogram. In Figs. 3(c) and 3(d), we show the Pt-ODT-Pt case. We observed the low conductance (LC), medium conductance (MC), and high conductance (HC) series in both configurations more clearly in the divided histograms, Figs. 3(b) and 3(d). From the results of Fig. 3, we can measure more precisely the locations of MC and HC. We also find a new series of conductance peaks not clearly visible in the original histogram, which we denote the LC (low conductance) series. We note that we used logarithmic binning (100 bins per decade) in Figs. 3(b) and 3(d) to keep the density of points constant on the logarithmic conductance axis. Ordinary linear histogram bins gave similar results, albeit with more noise at high frequencies.

B. Three series of conductances

We list the inferred conductance values in Table I. The conductance value for Pt-ODT-Pt is highest, followed by that of Pt-ODT-Au, and then Au-ODT-Au. The conductance values for Pt electrodes are about 2 to 2.5 times higher to those

on Au, showing the significant influence of the electrode material.[10,39,44,50,57] Pt-ODT-Au conductance values were intermediate but closer to the values for Au-ODT-Au.

Table I shows that the ratio between primary conductances (HC:MC and MC:LC) for Au-ODT-Au ≈ 5, consistent with previous results.[17,22,44] The Pt-ODT-Pt and Pt-ODT-Au conductance series show similar or somewhat smaller ratios.

IV. DISCUSSION

The existence of three series of conductances (LC, MC, and HC) has been previously observed in the Au-ODT-Au system.[17,18,22] Let us discuss three hypotheses on the origin of the LC series:

Li *et al.*[22] observed the third LC series in ODT and nonanedithiol (C9) systems. They attributed the LC series to a conformational change of a single molecule (*trans-gauche* isomer). In the *gauche* conformation, conductance values are predicted to be lower than that for *trans* isomer, as they observed. However, if the LC series were the result of isomerization, we would observe increasing currents as the tip was withdrawn, since we would expect the *gauche* isomer to straighten into the *trans* isomer.[42,43] However, in current-distance traces such as the ones shown in Figs. 2(b)–2(d), we saw no evidence for such a conductance increase.

Another possibility for the LC series is that ODT molecules can form a dimer. A gold atom between two ODT molecules can hop off the lattice and form Au-ODT-Au-ODT-(Au or Pt), since Au-S binding is stronger than Au-Au binding. Cossaro *et al.*[58] suggest that a gold atom that connects two thiol ligands can easily hop off the lattice. Thus, in the break-junction process, a dimer of ODT with a gold atom can form. Such a dimer could show half, or less than half, of the conductance of MC, which would correspond to LC. But if the same analogy is applied to the Pt-ODT-Pt system, a Pt atom should also come off the lattice as a result of the binding force of two thiol ligands. However, in contrast to the Au-thiol case, the Pt-Pt binding energy is much greater than the Pt-S binding energy,[59,60] making it unlikely that a Pt atom would hop off the surface to form a dimer-like configuration such as Pt-ODT-Pt-ODT-Pt.

A third possibility has been suggested by Haiss *et al.*,[16–19] who used the "$I(s)$ method," a technique similar to the break-junction method. They also observed three series of conductances and attributed them to the different distances between electrodes for a molecule that connects the electrodes in three configurations (edge-edge, top-edge, top-top).[17–19] They observed that conductances are smaller when the distance between STM tip and substrate is large and showed that the three distinct conductance series correspond to three distinct gap distances. In addition, Zhou *et al.*[25–30] observed four series of conductance values in the Au-ODT-Au system in a modified break-junction system. The values depended on the molecular configurations, which varied when the distance between the electrodes was mechanically oscillated. Both observations are similar to our observation of three conductances.

From the conductance values of MC and HC of ODT, we observe that HC values were 5 times higher than MC in the Au-ODT-Au system, as had been previously observed for
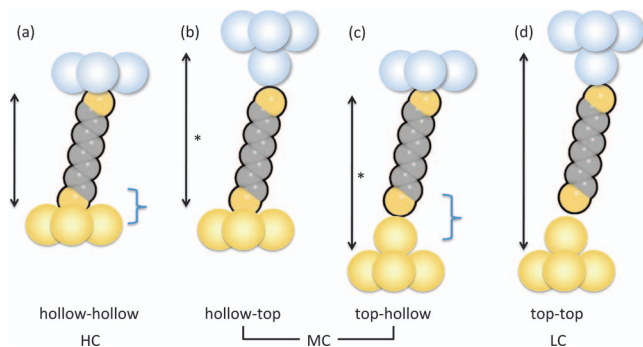
FIG. 4. Two possible substrate binding sites implies three conductances. The distance between electrodes affects the binding force, and the number of involved electrons for charge transport should determine the conductance of the metal-molecule-metal system. Double arrows indicate transport lengths for (a) hollow-hollow (b), (c) hollow-top/top-hollow, and (d) top-top. The hollow-top/top-hollow lengths (*) are equal.

Au-ODT-Au and attributed to binding structure.[34,44,57] Likewise, we observed that the MC conductance is also about 5 times higher than that of the LC in the Au-ODT-Au system. We, therefore, propose that these three conductance series result from three possible binding configurations between Pt or Au electrodes and thiol ligands, as illustrated in Fig. 4. In detail, the conductance value of the top-hollow configuration corresponds to MC. Similarly, we associate LC with the peak found using the control experiments. The schematic binding geometries for the HC, MC, and LC series are hypothesized to be as shown in Fig. 4. Recent theoretical studies propose that bridge binding (a thiol binding with two gold atoms) is more stable than hollow binding (a thiol binding with three gold atoms).[61] If we substitute the hollow configuration for the bridge configuration, it is still possible to form three configurations similar to Fig. 4, and the conductance values remain compatible with our hypothesis, where two gold atoms bind to a thiol ligand from the molecule, allowing bridge-bridge, bridge-top, and top-top configurations.[61]

Our results suggest that the conductance mechanisms at the interface depend greatly on the binding configuration. As argued above, the three conductance series correspond to three binding configurations and not to isomerization of the molecule. The differences among conductances in the different binding configurations then depend on the number of electron channels that a thiol ligand can contact in the molecule. Since the MC configuration has three times more channels for an electron to flow through than does the LC, its conductance value is correspondingly higher. We can apply the same analogy to the HC configuration[44] and to the Pt electrode, where each Pt atom has two electron transport channels (σ, π). Since the conductance ratio from MC to LC (HC to MC) is not two or three but five, the conductance at the interface is not solely determined by the number of electron channels that the ligand contacts. In addition, the ODT conductance at the Pt electrode is more than two times that of Au, even though π binding contributes only about 10% of the charge transport at the Pt electrode.[39]

Thus, there must be another contribution to the conductance beyond the number of electron channels. One possible explanation for the additional contribution is that, near the Fermi energy, the density of states for Pt is significantly higher (by a factor of ≈ 8) than for Au.[62] Even though those states are dominated by d orbitals, they can lead to resonances within the HOMO-LUMO gap that arise from their hybridization with sulfur. These states then contribute significantly to the conductance at low bias.[24,37]

V. CONCLUSIONS

In summary, we have introduced a method to effectively remove the background from conductance histograms of metal-molecule-metal systems that use the complicated but technologically important thiol linker. With this technique, we have investigated the interface conductance properties between ODT molecules and Au and Pt electrodes. We have observed a third series, LC, which corresponds to top-top bond configurations, while the HC and MC series correspond to the hollow-hollow and hollow-top configurations. The observed conductance values depend on both the number of electron channels and on the density of states near the Fermi level of the substrate metal.

A more complete understanding of the charge-transport mechanisms at the metal-molecule interfaces requires more extensive investigation. It would be interesting to do measurements at various bias voltages, in order to clarify the role of electronic states at the Pt electrode interface. Similarly, one should measure I-V curves for a single metal-molecule-metal system to analyze energy states (such as IETS) for the given metal-molecule-metal configurations. Finally, the background-removal method described here may prove valuable in further studies of systems using strongly bonding ligands.

[1] A. Aviram and M. A. Ratner, Chem. Phys. Lett. **29**, 277 (1974).
[2] R. L. Carroll and C. B. Gorman, Angew. Chem., Int. Ed. Engl. **41**, 4378 (2002).
[3] S. Kelley, N. Jackson, M. Hill, and J. Barton, Angew. Chem., Int. Ed. Engl. **38**, 941 (1999).
[4] S. H. Choi, B. Kim, and C. D. Frisbie, Science **320**, 1482 (2008).
[5] E. G. Emberly and G. Kirczenow, Phys. Rev. B **64**, 235412 (2001).
[6] R. E. Holmlin, R. Haag, M. L. Chabinyc, R. F. Ismagilov, A. E. Cohen, A. Terfort, M. A. Rampi, and G. M. Whitesides, J. Am. Chem. Soc. **123**, 5075 (2001).
[7] M. A. Reed, C. Zhou, C. J. Muller, T. P. Burgin, and J. M. Tour, Science **278**, 252 (1997).
[8] B. Xu and N. J. Tao, Science **301**, 1221 (2003).
[9] B. Xu, X. Xiao, and N. J. Tao, J. Am. Chem. Soc. **125**, 16164 (2003).
[10] V. B. Engelkes, J. M. Beebe, and C. D. Frisbie, J. Am. Chem. Soc. **126**, 14287 (2004).
[11] X. Cui, A. Primak, X. Zarate, J. Tomfohr, O. Sankey, A. Moore, T. Moore, D. Gust, G. Harris, and S. Lindsay, Science **294**, 571 (2001).
[12] A. Nitzan and M. A. Ratner, Science **300**, 1384 (2003).
[13] N. J. Tao, Nat. Nanotechnol. **1**, 173 (2006).
[14] J. C. Love, L. A. Estroff, J. K. Kriebel, R. G. Nuzzo, and G. M. Whitesides, Chem. Rev. **105**, 1103 (2005).
[15] L. Venkataraman, J. E. Klare, I. W. Tam, C. Nuckolls, M. S. Hybertsen, and M. L. Steigerwald, Nano Lett. **6**, 458 (2006).

[16]W. Haiss, R. Nichols, H. V. Zalinge, S. Higgins, D. Bethell, and D. Schiffrin, Phys. Chem. Chem. Phys. **6**, 4330 (2004).

[17]W. Haiss, S. Martin, E. Leary, H. V. Zalinge, S. J. Higgins, L. Bouffier, and R. J. Nichols, J. Phys. Chem. C **113**, 5823 (2009).

[18]W. Haiss, S. Martin, L. E. Scullion, L. Bouffier, S. J. Higgins, and R. J. Nichols, Phys. Chem. Chem. Phys. **11**, 10831 (2009).

[19]R. Nichols, W. Haiss, S. Higgins, E. Leary, S. Martin, and D. Bethell, Phys. Chem. Chem. Phys. **12**, 2801 (2010).

[20]W. Haiss, H. V. Zalinge, S. J. Higgins, D. Bethell, H. Höbenreich, D. J. Schiffrin, and R. J. Nichols, J. Am. Chem. Soc. **125**, 15294 (2003).

[21]J. M. Beebe, B. Kim, J. W. Gadzuk, C. D. Frisbie, and J. G. Kushmerick, Phys. Rev. Lett. **97**, 026801 (2006).

[22]C. Li, I. Pobelov, T. Wandlowski, A. Bagrets, A. Arnold, and F. Evers, J. Am. Chem. Soc. **130**, 318 (2008).

[23]C. Kaun and T. Seideman, Phys. Rev. B **77**, 033414 (2008).

[24]H. Dalgleish and G. Kirczenow, Nano Lett. **6**, 1274 (2006).

[25]K. Müller, Phys. Rev. B **73**, 045403 (2006).

[26]B. Xu, Small **3**, 2061 (2007).

[27]J. Zhou, F. Chen, and B. Xu, J. Am. Chem. Soc. **131**, 10439 (2009).

[28]J. Zhou, G. Chen, and B. Xu, J. Phys. Chem. C **114**, 8587 (2010).

[29]J. Zhou and B. Xu, Appl. Phys. Lett. **99**, 042104 (2011).

[30]J. Zhou, C. Guo, and B. Xu, J. Phys.: Condens. Matter **24**, 164209 (2012).

[31]K. Horiguchi, M. Tsutsui, S. Kurokawa, and A. Sakai, Nanotechnology **20**, 025204 (2009).

[32]X. Xiao, B. Xu, and N. J. Tao, Nano Lett. **4**, 267 (2004).

[33]M. Kamenetska, M. Koentopp, A. C. Whalley, Y. S. Park, M. L. Steigerwald, C. Nuckolls, M. S. Hybertsen, and L. Venkataraman, Phys. Rev. Lett. **102**, 126803 (2009).

[34]F. Chen, X. Li, J. Hihath, Z. Huang, and N. Tao, J. Am. Chem. Soc. **128**, 15874 (2006).

[35]Y. S. Park, A. C. Whalley, M. Kamenetska, M. L. Steigerwald, M. S. Hybertsen, C. Nuckolls, and L. Venkataraman, J. Am. Chem. Soc. **129**, 15768 (2007).

[36]E. Adaligil, Y.-S. Shon, and K. Slowinski, Langmuir **26**, 1570 (2010).

[37]H. Dalgleish and G. Kirczenow, Phys. Rev. B **73**, 245431 (2006).

[38]M. Kiguchi, S. Miura, K. Hara, M. Sawamura, and K. Murakoshi, Appl. Phys. Lett. **91**, 053110 (2007).

[39]C.-H. Ko, M.-J. Huang, M.-D. Fu, and C.-H. Chen, J. Am. Chem. Soc. **132**, 756 (2010).

[40]A. Salomon, D. Cahen, S. Lindsay, J. Tomfohr, V. B. Engelkes, and C. D. Frisbie, Adv. Mater. **15**, 1881 (2003).

[41]J. Ulrich, D. Esrail, W. Pontius, L. Venkataraman, D. Millar, and L. Doerrer, J. Phys. Chem. B **110**, 2462 (2006).

[42]M. Fujihira, M. Suzuki, S. Fujii, and A. Nishikawa, Phys. Chem. Chem. Phys. **8**, 3876 (2006).

[43]A. Nishikawa, J. Tobita, Y. Kato, S. Fujii, M. Suzuki, and M. Fujihira, Nanotechnology **18**, 424005 (2007).

[44]X. Li, N. Tao, and S. Lindsay, J. Am. Chem. Soc. **128**, 2135 (2006).

[45]S. Csonka, A. Halbritter, G. Mihaly, E. Jurdik, O. I. Shklyarecskii, and H. van Kempen, Phys. Rev. Lett. **90**, 116803 (2003).

[46]N. Prokopuk, K.-A. Son, and C. Waltz, J. Phys. Chem. C **111**, 6533 (2007).

[47]H. Song, H. Lee, and T. Lee, J. Am. Chem. Soc. **129**, 3806 (2007).

[48]K. Slowinski, R. Chamberlain II, R. Bilewicz, and M. Majda, J. Am. Chem. Soc. **118**, 4709 (1996).

[49]K. Slowinski, R. Chamberlain, C. Miller, and M. Majda, J. Am. Chem. Soc. **119**, 11910 (1997).

[50]M. S. Hybertsen, L. Venkataraman, J. E. Klare, A. C. Whalley, M. L. Steigerwald, and C. Nuckolls, J. Phys.: Condens. Matter **20**, 374115 (2008).

[51]S.-Y. Jang, P. Reddy, A. Majumdar, and R. A. Segalman, Nano Lett. **6**, 2362 (2006).

[52]J. R. Widawsky, M. Kamenetska, J. Klare, C. Nuckolls, M. L. Steigerwald, M. S. Hybertsen, and L. Venkataraman, Nanotechnology **20**, 434009 (2009).

[53]D. Wold and C. Frisbie, J. Am. Chem. Soc. **123**, 5549 (2001).

[54]V. B. Engelkes, J. M. Beebe, and C. D. Frisbie, J. Phys. Chem. B **109**, 16801 (2005).

[55]V. B. Engelkes and C. D. Frisbie, J. Phys. Chem. B **110**, 10011 (2006).

[56]Y. Qi, I. Ratera, J. Y. Park, P. D. Ashby, S. Y. Quek, J. B. Neaton, and M. Salmeron, Langmuir **24**, 2219 (2008).

[57]T. Morita and S. Lindsay, J. Am. Chem. Soc. **129**, 7262 (2007).

[58]A. Cossaro, R. Mazzarello, R. Rousseau, L. Casalis, A. Verdini, A. Kohlmeyer, L. Floreano, S. Scandolo, A. Morgante, M. L. Klein, and G. Scoles, Science **321**, 943 (2008).

[59]D. Karhánek, T. Bučko, and J. Hafner, J. Phys.: Condens. Matter **22**, 265006 (2010).

[60]D. Karhánek, T. Bučko, and J. Hafner, J. Phys.: Condens. Matter **22**, 265005 (2010).

[61]F. Demir and G. Kirczenow, J. Chem. Phys. **134**, 121103 (2011).

[62]D. A. Papaconstantopoulos, *Handbook of the Band Structure of Elemental Solids* (Plenum, New York, 1986).